

Reactor Power Distribution Calculation in Research Reactors Using MCNPZeyun Wu^{1,2*} and Robert E. Williams¹¹*NIST Center for Neutron Research, 100 Bureau Drive, Mail Stop 6101, Gaithersburg, MD 20899 USA*²*Department of Materials Science and Engineering, University of Maryland, College Park, MD 20742 USA***Corresponding author: zeyun.wu@nist.gov***INTRODUCTION**

In reactor calculations, a detailed 3-D power density distribution is required for core optimization studies and safety analyses. The general Monte Carlo based neutral particle transport tool, MCNP [1], has the capability to obtain detailed power density distribution in a reactor through its criticality calculation mode (KCODE mode). However, there is no standard tally type in MCNP that is able to directly provide total power information (F7 tally only accounts for prompt energy release in fission.). Moreover, because tally results obtained from MCNP are normalized to either fixed source strength (fixed source mode calculation) or total active fission source (k -eigenvalue mode calculation), some additional efforts are inevitably required to obtain the absolute power factors in the reactor.

Power density for a given position in a core is essentially determined by the effective recoverable fission energy deposited in the position. The majority of the fission energy appears as kinetic energy of the fission fragments and is deposited at the point of fission. Over 90% of the recoverable fission energy is deposited directly in the fissile material [2]. In power density calculations with MCNP, we conservatively assume that all the recoverable fission energy is deposited at the point of fission, and the power density is proportional to fission density. Thus the power factors of a position are directly proportional to the fission density at that position. If the power and fuel volume is known, the averaged power density among the fuels can be calculated. Therefore the power density can be obtained by the product of the average power density and the local power factor. With these considerations, the remaining task for power density calculation is to obtain fission density of points under interest.

METHODS FOR POWER DENSITY CALCULATION IN MCNP

This summary presents two alternative methods to generate detailed 3-D fission density distribution in a core by using different features provided in MCNP. The first method (referred to as FMESH method thereafter) applies flux tally (F4 card) or mesh flux tally (FMESH card) and tally multiplication option (FM card) in MCNP to produce cell-wise fission density value. The superimposed mesh tally capability provides significant convenience for the

calculation. Use of cell-wise flux tally to obtain fission density is not new to many experienced MCNP users and it works as a standard method to estimate power density in reactor calculations [3-4].

The second method (referred to as Table128 method thereafter), however, is not very familiar to most users, but it is noteworthy because it does not need any standard tally results to produce power density values, thereby greatly reducing the effort in preparing problem inputs [5]. This method uses converged fission source number printed in the universe map table (Table 128) in the standard output of MCNP. The original purpose of Table 128 is to provide users an optional diagnostic to quantitatively check fission sampling situation in cells containing fissionable materials. As a result, the converged fission neutron source number will be printed for every cell containing fissionable material in a reliable calculation. The fission source number of a cell is naturally proportional to the fission density in that cell. If statistical requirements are satisfied, these fission source numbers can be used to infer the fission density information. As Table 128 can be written to the output file without any extra input efforts, it actually provides a straightforward way to obtain power density information in MCNP. It is not printed as default by MCNP and must be triggered by PRINT card.

Both methods introduced above have relative strengths and defects. The FMESH method can theoretically produce fission density at arbitrary meshes, especially when using superimposed mesh tally, but it requires additional mesh definition and computational cost for flux tallies. The post data processing is relatively easier as the hierarchy of output results can be controlled and organized by MCNP. The Table 128 method is straightforward and no additional computations are required, but cells containing fissionable materials need to be divided into multiple sub cells if detailed power density is desired as converged fission source number is only available in real cells. More effort is usually required for post data processing in Table 128 method. However, the power density resulting from both methods are in excellent agreement, which is certainly true as either method basically performs identical Monte Carlo calculation and generate power density based on simulation of same amount of particles.

The following section presents a problem on power density calculation of a research reactor. The point of the example is to provide a model case to show how the power

density information can be obtained by employing the two methods described above, and also demonstrate the equivalence of the results yielded from these two methods.

EXAMPLE AND RESULTS

To demonstrate the power density calculation methods described above, a research reactor, which is analogue to Australia's OPAL reactor [6-7], is modeled with MCNP6 for this work. OPAL is a high flux performance reactor designed principally for radioisotope production and neutron beam experiments. Its compact core is surrounded with a heavy water reflector. The core consists of 16 fuel elements of square cross-section and is cooled and moderated by light water. A schematic view of the reactor model is shown in Fig. 1 and a close view of the core layout with 16 fuel elements and water channel box frame is shown in Fig. 2. The OPAL geometry was just one of the compact cores studied for a conceptual design of a new research reactor for NIST.

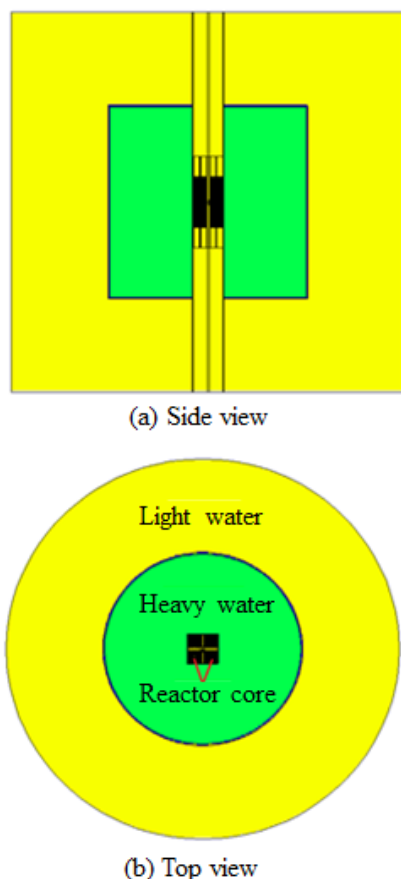


Fig. 1. A schematic view of cutaway side-plane (a) and mid-plane (b) of the reactor.

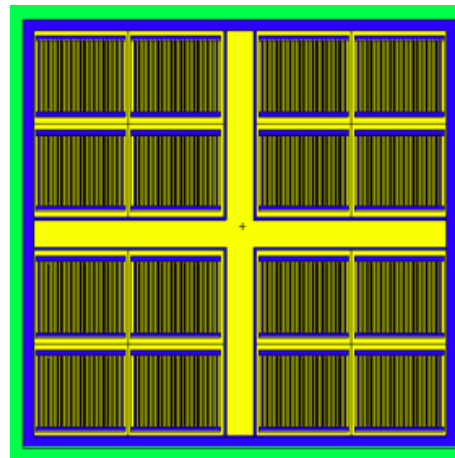


Fig. 2. Fuel elements scheme in the core layout

The fuel elements are configured in a symmetric 4 x 4 scheme in the core. The gaps in the center of the core are the space left for control elements not modeled here. An equilibrium end of cycle (EOC) fuel inventory is generated via the PRELIM method [8] and used in the model for power density calculation. The fuel element consists of 17 MTR (Materials Test Reactor) type fuel plates. Each fuel plate has LEU (19.7%) U_3Si_2 fuel meat in aluminum cladding. For simplicity, the fuel plate is modeled as a rectangular shape with the fuel meat dimension as 60 cm long, 6.134 cm wide, and 0.066 cm (26 mil) thick.

To obtain detailed 3-D fission density behavior in the core, the regions containing fissionable material need to be discretized into sub-cells or nodes. For this problem, the fuel meat is divided into 30 nodes in length, 3 nodes in width, and 1 node in thickness, thus the number of computational nodes in one fuel plate is $30 \times 3 \times 1 = 90$ with the volume 0.2699 cm^3 for each node. Taking into account of the number of plates and the number of fuel elements in the core, the total number of fissionable nodes in the example is $90 \times 17 \times 16 = 24480$. Since the fuel has 30 segments in axial direction, the results will be better presented as 30 axial levels with 12×68 nodes in each level.

The above discretized scheme is applied to both methods discussed previously. Fig. 3 depicts the X-Y 2D nodal power distribution of the hottest plane ($Z = 16$) from these two methods. Note here the superimposed meshes in the FMESH tallies are also defined with the identical boundaries as the nodes in the Table128 method, although theoretically they can be defined at any arbitrary size.

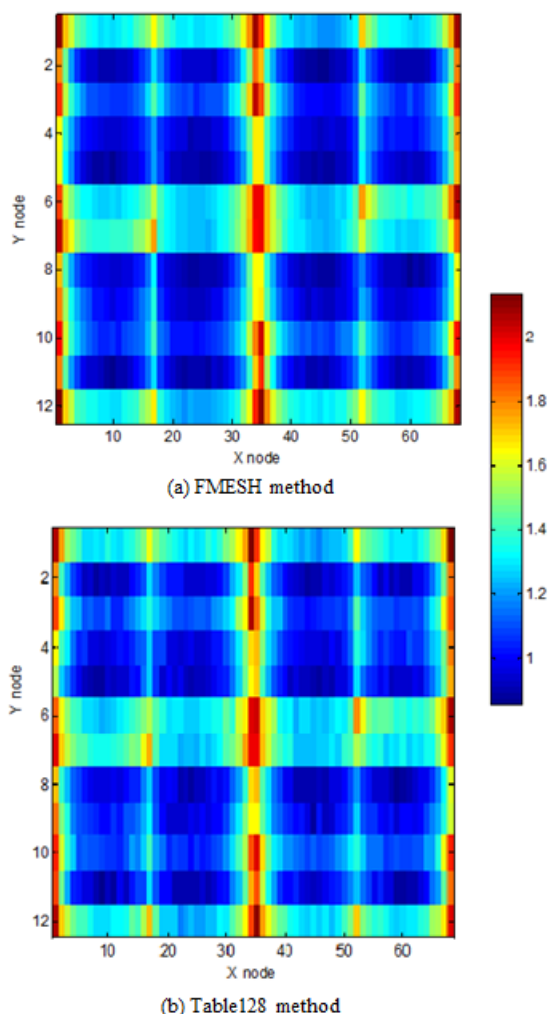


Fig. 3. Planar power density distribution in the hottest plane obtained from both methods.

As shown in Fig. 3, the results yielded from both methods are almost identical and all the relative high power spots occur at the plates either in the side or in the corner of the core. Table 1 presents the twelve hottest node positions and power factors identified by both methods. The statistical error for FMESH method is directly provided by MCNP output, while the one for Table128 method is calculated based on standard statistics [9] with the assumption that the standard deviation of the data in Table 128 is the square root of the number. It can be seen that the *standardized differences* (i.e., the *z-factors*) between the results of both methods are all less than 1.63. The *z-factor* is conventionally used as a measure of accuracy between statistic quantities. It is defined as follows [10]:

$$z - factor = \frac{|x_1 - x_2|}{\sqrt{\sigma_1^2 + \sigma_2^2}} \quad (1)$$

where x_1 and x_2 are two statistic variables, σ_1 and σ_2 are the standard deviations associated with them. In general, if the *z-factor* is < 2 , the difference between two statistic values are acceptable. The maximum power factor in the nodes obtained from both methods are 2.136 and 2.139, respectively. They do not occur in the same position in different method (see Table I), but the difference is acceptable as explained above and also with the consideration the statistical nature of Monte Carlo calculation.

Table I. Comparison of power factor of some hot spots in the mid-plane of the core

X	Y	FMESH	Table128	<i>z-factor</i>
1	1	2.100±0.025	2.072±0.032	0.689
34	1	2.077±0.023	2.139±0.032	1.573
35	1	1.917±0.021	1.916±0.031	0.027
68	1	2.081±0.025	2.132±0.032	1.256
1	6	1.889±0.021	1.841±0.030	1.311
34	6	1.988±0.019	2.005±0.031	0.468
35	6	1.979±0.019	2.034±0.032	1.478
68	6	2.073±0.023	2.066±0.032	0.178
1	7	2.047±0.023	2.012±0.031	0.907
34	7	1.975±0.019	1.996±0.031	0.578
35	7	1.991±0.019	1.979±0.031	0.330
68	7	1.856±0.021	1.908±0.031	1.389
1	12	2.136±0.026	2.069±0.032	1.625
34	12	1.937±0.021	1.892±0.030	1.229
35	12	2.101±0.023	2.106±0.032	0.126
68	12	2.062±0.024	1.999±0.031	1.607

For a better comparison, all 816 power factors radially shown in Fig. 3 are plotted in Fig. 4. The 2D planar power factors in the hottest plane yielded from both methods are plotted into 1D lines with the comparison of the statistical errors and deviations of both methods. Figure 4 clearly shows the deviations of both methods stay in the same level as the statistical errors, which indicates the results yielded from these different methods are statistically identical.

Fig. 5 presents the axial power distribution of the hottest channel obtained from both methods in the similar way as the one in Fig. 4. It simply shows that the axial power distribution from both methods are in an excellent agreement.

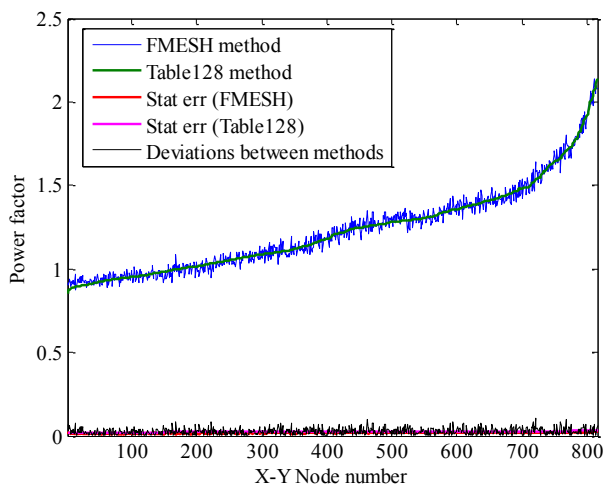


Fig. 4. Comparison of X-Y (hottest plane) node power density obtained from both methods

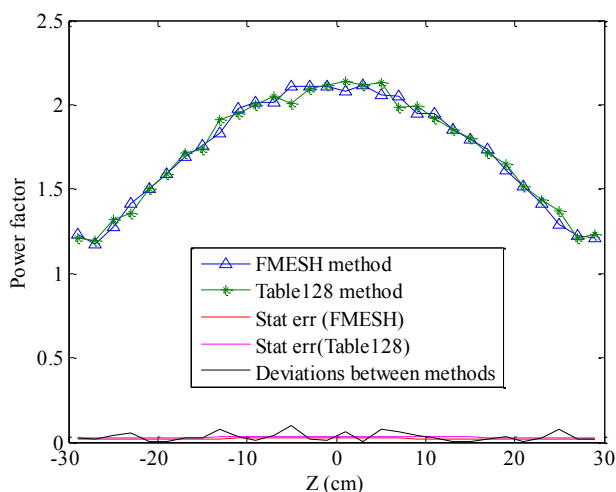


Fig. 5. Comparison of axial power density (hottest channel) obtained from both methods

CONCLUSION

This paper summarizes two alternative easily applied methods for power density estimation in nuclear reactor calculations using the MCNP code. One method uses information provided by superimposed mesh tally (FMESH card). The other one uses information provided in the universe map table (Table 128). Our experience on an example problem shows that these two methods can produce statistically identical reactor power density distributions for the core. However, additional efforts are

required in both methods, either in the modeling or in data post processing procedure. Different methodologies need to be applied in the calculation of the normalization factor for the purpose of obtaining physically equivalent quantities.

REFERENCES

1. D.B. PELOWITZ, Ed., "MCNP6 User's Manual," LA-CP-11-01708, Los Alamos National Laboratory, December (2012).
2. J. J. DUDERSTADT and L. J. HAMILTON, *Nuclear Reactor Analysis*, John Wiley & Sons, (1976).
3. L. SNOJ and M. RAVNIK, "Calculation of Power Density with MCNP in TRIGA Reactor," *Proceedings of the International Conference Nuclear Energy for New Europe*, Nuclear Society of Slovenia (2006).
4. G. ŽEROVNIK, M. PODVRATNIK, and L. SNOJ, "On Normalization of Fluxes and Reaction Rates in MCNP Criticality Calculations," *Annals of Nuclear Energy*, **63**, 126-128 (2014).
5. A. L. HANSON and D. J. DIAMOND, "Calculation of Design Parameters for an Equilibrium LEU Core in the NBSR", Brookhaven National Laboratory, BNL-96386-2011-IR, Sept. (2011).
6. R. MILLER and P. M. ABBATE, "Australia's New High Performance Research Reactor," *the 9th Meeting of the International Group on Research Reactors (IGORR-9)*, Sydney, Australia, March 24-28 (2003).
7. S. KIM, "The OPAL (Open Pool Australian Light-water) Reactor in Australia", *Nuclear Engineering and Technology*, **39**(5), 443-448, Special issue on HANARO (2005).
8. Z. WU and R. WILLIAMS, "A Fast and Self-consistent Method for Multi-cycle Equilibrium Core Studies Using Monte Carlo Models", *the Joint International Conference on Mathematics and Computation (M&C), Supercomputing in Nuclear Applications (SNA) and the Monte Carlo (MC) Method*, Nashville, TN, USA, April 19-23, on CD-ROM (2015).
9. A. PAPOULIS and S. PILLAI, *Probability, Random Variables, and Stochastic Processes*, McGraw-Hill (2002).
10. P. BODE and C. P. VAN DIJK, "Operational Management of Results in INAA Utilizing a Versatile System of Control Charts," *Journal of Radioanalytical and Nuclear Chemistry*, **215**(1), 87-94 (1997).